4-2001

Infrared Spectroscopy Of H-bonded Bridges Stretched Across The Cis-amide Group: I. Water Bridges

Joel R. Carney

A. V. Fedorov

John R. Cable
Bowling Green State University, cable@bgsu.edu

Timothy S. Zwier

Infrared Spectroscopy of H-Bonded Bridges Stretched across the *cis*-Amide Group: I. Water Bridges

Joel R. Carney,[†] A. V. Fedorov,[‡] J. R. Cable,*[,‡] and Timothy S. Zwier*[,†]

Department of Chemistry, Purdue University, 1393 Brown Laboratory, West Lafayette, Indiana 47907-1393, and Department of Chemistry and Center for Photochemical Sciences, Bowling Green State University, Bowling Green, Ohio 43403-0213

Received: September 18, 2000; In Final Form: January 9, 2001

The water-containing clusters of oxindole (OI) and 3,4-dihydro-2(1*H*)-quinolinone (DQ) have been studied in the hydride stretch region of the infrared by the technique of resonant ion-dip infrared spectroscopy (RIDIRS). Both OI and DQ are constrained *cis*-amides with adjacent N−H and C═O groups between which water can form H-bonded bridges. The hydride stretch fundamentals of OI−W_n with $n = 1-3$ and DQ−W_n with $n = 1, 2$ without exception divide up into free OH stretch fundamentals near 3700 cm^{-1} and a set of H-bonded bridge fundamentals in the 3200−3450 cm^{-1} region. The bridge fundamentals show a distribution of intensities that reflects strong coupling among the XH oscillators in the bridge. When more than one water is involved in the bridge, the bridge fundamentals are unusually broad, with widths of 50−80 cm^{-1} full width at half-maximum. Minimum-energy structures, binding energies, vibrational frequencies, and infrared intensities have been calculated by density functional theory with a Becke3LYP functional and a 6-31+G* basis set. The calculated infrared spectra match experiment well, confirming the bridge structures for the clusters. The form of the calculated normal modes provides insight into the nature of the bridge fundamentals.

I. Introduction

In seeking a molecular-scale understanding of water's interactions with the amide group, the study of solute−$(water)_n$ clusters formed in a supersonic expansion offers a unique vantage point in which the most stable H-bonded structures taken up by the first few water molecules can be explored in a size- and conformation-specific manner.[1] In bulk solution, the influence of water solvation on the amide linkage has been extensively studied.[2,3] In solution, the amide vibrational frequencies and intensities are influenced both by the dielectric effect of the solvent and by H-bonding of specific solvent molecules with the N−H and C═O groups of the amide moiety.[2,3] By studying the water-containing clusters of amides in the gas phase, free from the influence of the surrounding dielectric, the effects of bound water can be distinguished from those due to the bulk dielectric. In most circumstances, the amide linkage prefers a trans configuration that points the two H-bonding sites (N−H and C═O) in opposite directions,[4] preventing a single water molecule from interacting with both sites simultaneously. Illustrative of this is the recent work on the hydrated complexes of the trans isomer of formanilide (TFA).[5,6] However, the cis configuration places these groups side-by-side where water can easily bridge between them.

Several studies seeking to understand H-bonding to the *cis*-amide group have focused attention on 2-pyridone (2-PYR), which constrains the *cis*-amide group by incorporating it into a six-membered ring.[7−12]

Held and Pratt[9] have used high-resolution ultraviolet spectroscopy to prove that the water molecule(s) in 2-PYR−W_1 and 2-PYR−W_2 form H-bonded bridges between the N−H and C═O sites. The infrared spectroscopy of 2-PYR−W_1 and its deuterated analogues have been studied by Matsuda et al.[10] Our group has extended the infrared studies to include 2-PYR−W_2 and we have compared these results with the corresponding spectra of the 2-hydroxypyridine tautomer, which also forms water bridges.[12]

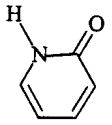

2-pyridone

One of the most striking features of the infrared spectra of the 2-PYR−W_n clusters is the unusual breadth of the H-bonded bridge hydride stretch fundamentals.[12] In the course of that study, several possible sources for the broadening were put forward. Among the most intriguing was the possibility that water-mediated tautomerization could contribute to the broadening, since excitation of the hydride stretch fundamentals provides an energy comparable to the calculated transition state for the tautomerization. Alternatively, the breadths could be a more general characteristic of H-bonded bridges with their cooperatively strengthened H-bonds. Finally, the breadths could be a peculiar feature of the *cis*-amide−$(water)_n$ bridges, in which the close proximity of the N−H and C═O groups squeezes the water dimer to unusually short separations ($R_{OO} < 2.7$ Å). In such circumstances, the coupling of the bridge XH bond stretches to the intermolecular bends and stretches of the water molecules could be enhanced.

To distinguish between these possibilities, and to study more systematically the spectroscopic consequences of forming water bridges to the *cis*-amide group, the present study focuses attention on the water-containing clusters of two constrained analogues of formanilide in which the *cis*-amide side chain is

* To whom correspondence should be addressed: T.S.Z. e-mail zwier@purdue.edu; J. R.Cable e-mail cable@bgnet.bgsu.edu.
† Purdue University.
‡ Bowling Green State University.

10.1021/jp003375f CCC: $20.00
Published on Web 03/21/2001

incorporated into a five-membered (oxindole, OI) or six-membered ring [3,4-dihydro-2(1*H*)-quinolinone, DQ]. In so

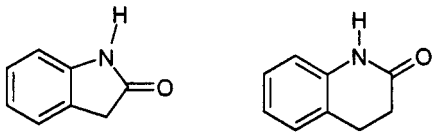

Oxindole (OI) 3,4-dihydro-2(1H)quinolinone (DQ)

doing, the separation between N−H and C═O groups can be systematically varied. As we shall see, incorporation of the *cis*-amide group into a six-membered ring in DQ produces an amide hydrogen−carbonyl oxygen separation of 2.45 Å, very similar to its value in 2-PYR. On the other hand, in OI, the five-membered ring opens the jaws of the *cis*-amide group to 2.63 Å.

The resonant two-photon ionization spectroscopy of these molecules and their clusters with water and ammonia have already been studied.[13] In that work, tentative structural deductions were drawn on the basis of the electronic frequency shifts of the cluster origins. The present paper extends that work to include resonant ion-dip infrared spectra of the water clusters of these amides, which provide a sensitive probe of the H-bonding environments present in the clusters.[1,14] We will report elsewhere[15] on the extension of these studies of OI and DQ to include ammonia and mixed ammonia−water bridges.

II. Experimental and Theoretical Methods

The resonant two-photon ionization (R2PI) and resonant ion-dip infrared (RIDIR) spectra of OI−W_n and DQ−W_n were recorded on a molecular beam time-of-flight mass spectrometer that has been described previously.[16,17] The latter technique enables the infrared spectrum of each cluster to be obtained free from interference from other species present in the expansion.[1,18−22] In RIDIRS, an ultraviolet laser is fixed on a vibronic transition of the cluster of interest, creating a steady-state ion signal of a given mass that reflects the ground-state population of the cluster. The infrared spectra were recorded by preceding the ultraviolet pulse with an infrared pulse that, when resonant with an infrared transition, removes population from the ground state. The absorption is then detected as a dip in the ion signal generated by the ultraviolet laser pulse that follows.

The OI−W_n and DQ−W_n molecular clusters are formed by expansion from a 0.8 mm diameter pulsed valve heated to 130 °C (for OI) or 160 °C (for DQ) and operating at a backing pressure of 2 bar. Typical water concentrations in the beam are 0.02% in Ne-70. The unfocused, doubled output of a Nd:YAG-pumped dye laser (with rhodamine 590 or a rhodamine 590/610 mix) is used as ultraviolet light source. Typical ultraviolet powers of 0.1−0.5 mJ/pulse were used in the R2PI spectra. For the RIDIR spectra, an infrared parametric converter pumped by the output of a second, seeded Nd:YAG laser was used for the infrared excitation step. The IR output counterpropagates the ultraviolet laser beam and is loosely focused by a 50 cm focal length lens to the center of the ion source region of the time-of-flight mass spectrometer. Typical infrared powers of about 5 mJ/pulse are used.

Density functional theory (DFT) calculations employing the Becke3LYP functional[23,24] with a 6-31+G* basis set[25] have been carried out to provide a basis of comparison with the experimental results. Fully optimized structures, binding energies, vibrational frequencies, and infrared intensities were computed for the hydrated complexes. Despite the close similarity of the RIDIR spectra of OI−W_n and DQ−W_n to one another and to those of 2-PYR−W_n (whose structures are known), H-bonded bridge structures were optimized for both OI−W_n and DQ−W_n clusters to give a more complete picture of the structural differences between them. Vibrational frequencies of optimized structures were performed in the harmonic approximation with analytical second derivatives. All calculations were carried out with the Gaussian 98 suite of programs.[26]

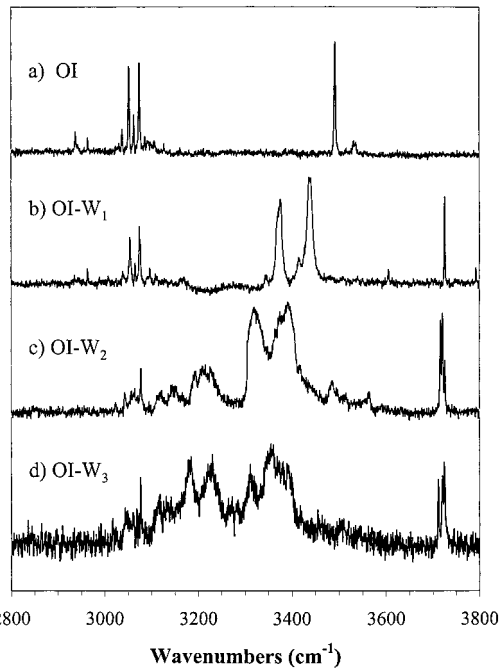

Figure 1. Overview RIDIR spectra for the water-containing clusters of oxindole: (a) oxindole monomer, (b) OI−W_1, (c) OI−W_2, and (d) OI−W_3. Shifts toward lower frequency in the hydrogen-bonded hydride stretch transitions highlight the strengthening of the bridge with the addition of each water molecule.

III. Results and Analysis

The R2PI spectroscopy of OI−W_n and DQ−W_n clusters has been studied previously.[13] The OI−W_n cluster $S_1 \leftarrow S_0$ origin transitions are shifted to the red of the OI monomer origin (34411 cm^{-1}) by −14, −70, and −101 cm^{-1} for $n = 1-3$, respectively. The analogous $S_1 \leftarrow S_0$ origin transitions in DQ−W_n are shifted +89 and +127 cm^{-1} to the blue from that of DQ monomer (34808 cm^{-1}). These transitions are used as monitor transitions in the RIDIR spectra of OI−W_n and DQ−W_n.

A. RIDIR Spectra. The RIDIR spectra of OI−W_n with $n = 1-3$ are shown in Figure 1 as spectra b−d, respectively. The OI monomer RIDIR spectrum (Figure 1a) is shown above them for comparison. The monomer spectrum consists of an NH stretch fundamental at 3493 cm^{-1}, a set of four aromatic CH stretch transitions at 3037, 3052, 3063, and 3074 cm^{-1}, and two weak alkyl CH stretch transitions due to the CH_2 group in the five-membered ring at 2938 and 2964 cm^{-1}. The weak band at 3532 cm^{-1} is tentatively assigned as the overtone of the carbonyl stretch.

The RIDIR spectra of OI−W_{1-3} (Figure 1b−d) show the general features anticipated for cluster structures in which the water molecule(s) form H-bonded bridges between the NH and C═O groups of the *cis*-amide. The NH and OH stretch transitions neatly divide into free OH stretch transitions (just above 3700 cm^{-1}) and H-bonded bridge fundamentals near 3400 cm^{-1} and below. The amide NH stretch fundamentals in the OI−W_n spectra are clearly shifted toward lower frequency relative to its position in OI monomer (3493 cm^{-1}) in response to formation of a H-bond to water. As the number of water

TABLE 1: Experimental Frequencies and Widths of the Observed RIDIR Transitions of OI−W_n (n = 0−3) and DQ−W_n (n = 0−2)

OI−W_n			DQ−W_n		
n	frequency (cm^{-1})	fwhm[a] (cm^{-1})	n	frequency (cm^{-1})	fwhm[a] (cm^{-1})
0	3493.0	3.5	0	3447.0	3.5
1	3725.5	2.0	1	3724.0	3.5
1	3437.5	13.0	1	3421.0	8.0
1	3375.5	14.0	1	3332.5	24.0
2	3726.0	3.0	2	3721.5	4.0
2	3721.0	3.5	2	3712.0	3.5
2	3717.0	3.0	2	3395.5	20.0
2	3393.5	52.5	2	3317.0	42.0
2	3320.0	45.5	2	3217.5	80.0
3	3724.5	4.0			
3	3720.5	4.0			
3	3711.5	3.0			
3	3355.5	70.0			
3	3311.5	21.0			
3	3230.5	35.0			
3	3184.5	24.0			

[a] Full width at half-maximum.

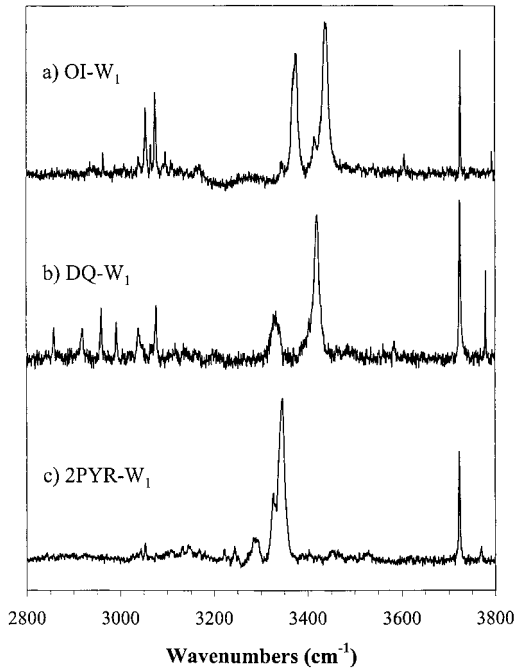

Figure 2. RIDIR spectra of the 1:1 water complex of three similar *cis*-amide groups: (a) OI−W_1, (b) DQ−W_1, and (c) 2PYR−W_1.

molecules in the OI−W_n cluster increases from one to three (Figure 1b−d), the bridge H-bonded stretch absorptions grow in complexity and breadth, and their center of gravity shifts to somewhat lower frequency. This indicates some cooperative strengthening of the XH stretch H-bonds in the bridge as the length of the bridge increases.[27] The frequencies, widths, and integrated intensities of the observed transitions in the RIDIR spectra are collected in Table 1.

Figure 2b shows the analogous RIDIR spectrum of DQ−W_1, juxtaposed with the corresponding spectra of OI−W_1 (Figure 2a) and 2-PYR−W_1 (Figure 2c) in order to highlight the similarities and differences between the spectra produced by the three *cis*-amide groups. As mentioned in the Introduction, the comparison of the DQ−W_n spectra to those of 2-PYR−W_n is particularly apt, since in both 2-PYR and DQ the *cis*-amide groups are incorporated into six-membered rings with nearly

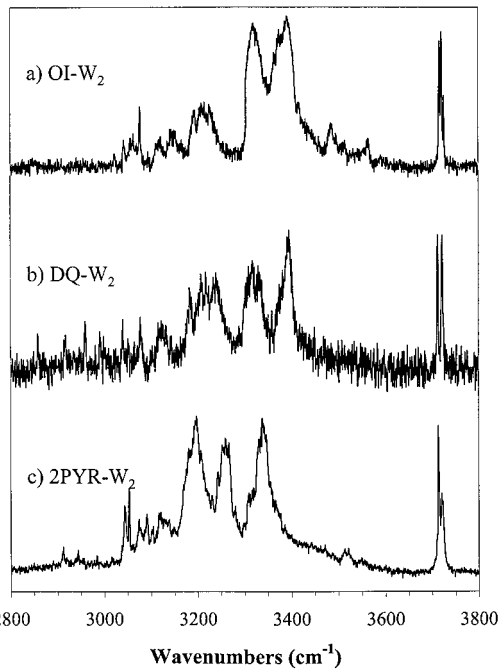

Figure 3. RIDIR spectra of the 1:2 water cluster of three similar *cis*-amide groups: (a) OI−W_2, (b) DQ−W_2, and (c) 2PYR−W_2.

identical separations between N−H and C═O groups. The 2-PYR−W_1 complex was studied recently by Matsuda et al.,[10] and 2-PYR−$W_{1,2}$ was studied by our group in the infrared.[12] It is known from the high-resolution ultraviolet spectroscopy of Held and Pratt[9] that the 2-PYR−W_n clusters with n = 1 and 2 incorporate the water molecule(s) in bridges between the N−H and C═O groups. The close similarity of the H-bonded bridge fundamentals of DQ−W_1 (Figure 2b) to those of 2-PYR−W_1 (Figure 2c) leaves little doubt that DQ−W_1 is also such a H-bonded bridge structure.

Figure 3 shows the analogous comparison of the spectrum of DQ−W_2 (Figure 3b) with those of OI−W_2 (Figure 3a) and 2-PYR−W_2 (Figure 3c). Once again, the close resemblance of the DQ−W_2 and OI−W_2 spectra to that of 2-PYR−W_2 provides strong evidence that the former clusters possess the same structure as the latter; namely, an H-bonded water dimer bridging the N−H and C═O groups.[9] All three spectra in Figure 3 also share in common the very large widths of the bridge fundamentals, which are some 50−100 cm^{-1} full width at half-maximum. Such widths, then, appear to be a general phenomenon associated with the water dimer bridge spanning the *cis*-amide group. Finally, the spectra of Figure 2 and 3 do show some differences in the relative intensities of the bridge fundamentals from one *cis*-amide group to the next. These differences reflect changes in the strength and coupling in the bridges. A further analysis of the infrared spectra of the water bridges will be taken up following discussion of the calculations.

B. Calculations. To understand these more subtle features of the spectra and to provide additional evidence for the structural assignments, DFT Becke3LYP/6-31+G* calculations[23−25] of the structures, vibrational frequencies, and infrared intensities of OI−W_n and DQ−W_n clusters have been carried out. Table 2 summarizes the key structural parameters of the OI monomer and OI−W_n clusters with n = 1−3, while Table 3 gives the analogous data for DQ and DQ−W_n, n = 1−2. Particular attention is paid in the tables to the structural parameters of the *cis*-amide group and the water bridges formed between them. The analogous structural data on the 2-PYR and 2-PYR−W_n clusters are given in the paper by Florio et al.[12]

TABLE 2: Structural Parameters and Binding Energies for the Calculated OI−W_n (n = 0−3) Minima Optimized at the B3LYP/6-31+G*(5d) Level of Theory

atomic separations[a] (Å)		angles[a] (deg)	
	OI		
NH	1.012	OCN	125.6
CO	1.219	CNH	121.8
NC	1.386	HNCO	0.1
(N)H−O(C)	2.631		
	OI−W_1[b]		
NH	1.021	OCN	125.4
W1 HB OH	0.984	CNH	120.4
W1 OH F	0.968	NHO_{W1}	135.9
CO	1.231	COO_{W1}	95.1
NC	1.372	$OH_{W1}O(C)$	148.2
$N(H)-O_{W1}$	2.827	HNCO	0.5
$O(H)_{W1}-O(C)$	2.805	$OCNO_{W1}$	0.2
$(N)H-O_{W1}$	2.003		
$(O)H_{W1}-O(C)$	1.920		
(N)H−O(C)	2.606		
	OI−W_2[c]		
NH	1.031	OCN	126.4
W1 HB OH	0.991	CNH	123.3
W1 OH F	0.969	NHO_{W1}	172.6
W2 HB OH	0.990	COO_{W2}	123.0
W2 OH F	0.968	$OH_{W1}O_{W2}$	162.1
CO	1.235	$OH_{W2}O(C)$	170.1
NC	1.366	HNCO	1.4
$N(H)-O_{W1}$	2.869	$OCNO_{W1}$	0.7
$O(H)_{W1}-O(H)_{W2}$	2.721	$OCNO_{W2}$	2.4
$O(H)_{W2}-OC$	2.762		
$(N)H-O_{W1}$	1.844		
$(O)H_{W1}-O_{W2}$	1.761		
$(O)H_{W2}-O(C)$	1.782		
(N)H−O(C)	2.667		
	OI−W_3[d]		
NH	1.031	OCN	126.6
W1 HB OH	0.993	CNH	124.8
W1 OH F	0.969	NHO_{W1}	190.6
W2 HB OH	0.993	COO_{W3}	136.9
W2 OH F	0.969	$OH_{W1}O_{W2}$	172.6
W3 HB OH	0.989	$OH_{W2}O_{W3}$	173.1
W3 OH F	0.969	$OH_{W3}O(C)$	177.0
CO	1.234	HNCO	1.4
NC	1.364	$OCNO_{W1}$	4.6
$N(H)-O_{W1}$	2.852	$OCNO_{W2}$	8.8
$O(H)_{W1}-O(H)_{W2}$	2.727	$OCNO_{W3}$	14.0
$O(H)_{W2}-O(H)_{W3}$	2.722		
$O(H)_{W3}-OC$	2.746		
$(N)H-O_{W1}$	1.833		
$(O)H_{W1}-O_{W2}$	1.739		
$(O)H_{W2}-O_{W3}$	1.734		
$(O)H_{W3}-O(C)$	1.758		
(N)H−O(C)	2.691		

[a] Atoms in parentheses are used to guide the reader in the specific atom designations and are not used as part of the calculated distances or angles. W1, W2, and W3 subscript labels describe atoms of specific water molecules, where the water molecules are numbered in the order they appear from the NH to the C═O group of oxindole. [b] Binding energy for OI−W_1 is 10.5 kcal/mol, or 8.0 kcal/mol with zero-point energy correction. [c] Binding energy for OI−W_2 is 24.0 kcal/mol, or 18.8 kcal/mol with zero-point energy correction. [d] Binding energy for OI−W_3 is 34.6 kcal/mol, or 27.0 kcal.mol with zero-point energy correction.

As noted in the Introduction, most of the bond distances and angles in the *cis*-amide groups of DQ and 2-PYR monomers are very similar to one another, as one would expect since both are constrained as part of six-membered rings. The only significant difference is the buckling of the six-membered ring in DQ, which produces an H−N−C═O dihedral angle of 4°. In OI, incorporation of the *cis*-amide group into a five-membered ring increases the size of the opening between the donor H on the NH and acceptor oxygen on the carbonyl from 2.45 to 2.63 Å [labeled (N)H−C(O) in the tables].

TABLE 3: Structural Parameters and Binding Energies for the Calculated DQ−W_n (n = 0−2) Minima Optimized at the B3LYP/6-31+G*(5d) Level of Theory

atomic separations[a] (Å)		angles[b] (deg)	
	DQ		
NH	1.014	OCN	121.3
CO	1.225	CNH	115.1
NC	1.380	HNCO	4.2
(N)H−O(C)	2.452		
	DQ−W_1[b]		
NH	1.023	OCN	121.8
W1 HB OH	0.985	CNH	115.6
W1 OH F	0.968	NHO_{W1}	143.2
CO	1.238	COO_{W1}	99.8
NC	1.367	$OH_{W1}O(C)$	149.5
$N(H)-O_{W1}$	2.893	HNCO	2.3
$O(H)_{W1}-O(C)$	2.772	$OCNO_{W1}$	2.3
$(N)H-O_{W1}$	2.008		
$(O)H_{W1}-O(C)$	1.879		
(N)H−O(C)	2.465		
	DQ−W_2[c]		
NH	1.030	OCN	122.5
W1 HB OH	0.991	CNH	117.9
W1 OH F	0.967	NHO_{W1}	175.7
W2 HB OH	0.990	COO_{W2}	128.4
W2 OH F	0.968	$OH_{W1}O_{W2}$	161.4
CO	1.241	$OH_{W2}O(C)$	170.1
NC	1.360	HNCO	2.4
$N(H)-O_{W1}$	2.899	$OCNO_{W1}$	0.7
$O(H)_{W1}-O(H)_{W2}$	2.717	$OCNO_{W2}$	1.7
$O(H)_{W2}-O(C)$	2.760		
$(N)H-O_{W1}$	1.870		
$(O)H_{W1}-O_{W2}$	1.759		
$(O)H_{W2}-O(C)$	1.780		
(N)H−O(C)	2.513		

[a] Atoms in parentheses are used to guide the reader in the specific atom designations and are not used as part of the calculated distances or angles. W1, W2, and W3 subscript labels describe atoms of specific water molecules, where the water molecules are numbered in the order they appear from the NH to the C═O group of DQ. [b] Binding energy for DQ−W1 is 10.5 kcal/mol, or 8.1 kcal/mol with zero-point energy correction. [c] Binding energy for DQ−W2 is 23.1 kcal/mol, or 17.9 kcal/mol with zero-point energy correction.

Several structural details in OI−W_1 indicate that the single water molecule cannot effectively span this opening between the donor and acceptor sites and thereby strains the H-bonds that are formed. These H-bonds are quite bent, with N−H···O and O−H···O angles of 136° and 148°, respectively. The N−H···O H-bond angle is about 7° further bent in OI−W_1 than in DQ−W_1, consistent with the larger (N)H−C(O) distance in the latter case. In OI−W_1, the single water bridge actually pulls in this distance by about 0.03 Å, but this does not occur appreciably in DQ−W_1.

When the bridge is extended by adding a second water molecule to it, the opposite circumstances apply; namely, that the water dimer is now slightly too big to comfortably span the *cis*-amide opening. The reader will recall that the most notable structural feature of the 2-PYR−W_2 cluster[9] is its unusually short O−O distance of R_2 = 2.67 Å. Here the *cis*-amide jaws squeeze the water dimer almost 0.3 Å closer together than its value in the free water dimer (2.98 Å).[28] In OI−W_2 and DQ−W_2, a similar squeezing of the dimer occurs, with computed $O_{W1}-O_{W2}$ distances of 2.72 Å for both clusters, compared to 2.70 Å for 2-PYR−W_2 (2.67 Å experimentally).[9] In fact, all the heavy-atom distances in the bridges for OI−W_2, DQ−W_2, and 2-PYR−W_2 are within 0.03 Å of each other, suggesting a

certain robustness of the bridge to modest changes in the donor−acceptor sites.

All the data in Table 2 are for the global minimum structure for OI−W_2, in which the free OH groups take up opposite sides of the heavy-atom plane (a so-called up/down structure).[12] This structure and its down/up analogue can be interconverted via a flipping coordinate that has a low barrier,[13] as it does in the free water trimer.[29,30] In previous work,[12] we have suggested that the observed splitting in the $S_1 \leftarrow S_0$ origin transition of 2-PYR−W_2[9] could be a tunneling splitting due to this flipping coordinate. In addition, there is a second minimum in OI−W_2, with an up/up configuration of the free OH groups. In 2-PYR−W_2, this structure is about 0.5 kcal/mol higher in energy.[12] As in 2-PYR−W_2, there is no experimental evidence for this structure in our spectra, which is probably annealed away by collisions in the expansion.

In OI−W_3, only the bridge structure was studied using DFT methods because only this structure is consistent with the qualitative appearance of the RIDIR spectrum. The recent study of Robertson et al.[31] on *N*-benzylformamide assigned their cis amide−W_3 cluster to an alternative structure, involving a cyclic water trimer with a doubly donating water molecule. The signature of this structure was a band at 3650 cm^{-1} in the infrared, which is not present in our data.

The addition of a third water molecule to the bridge forces more dramatic changes in the bridge structure in accommodating to the undersized opening it seeks to span (Table 2). The bridge does so by (i) sliding the NH-bound water slightly outside the opening (with a N−H···O_{W1} interior angle of 191°), and (ii) buckling the water bridge out-of-plane. In so doing, all the H-bond lengths and angles in the bridge are retained at near-optimum values while still enabling the terminal water molecules to bind strongly to the NH and C═O sites. Note that the distance between the NH hydrogen and carbonyl oxygen is stretched still further to 2.691, about 0.06 Å larger than in the monomer.

As Tables 2 and 3 indicate, the binding energies of OI−W_1 and DQ−W_1 are calculated to be virtually identical to one another (8.0 and 8.1 kcal/mol after ZPE correction), but significantly smaller than that for 2-PYR−W_1 (9.7 kcal/mol). Similarly, the total binding energies of OI−W_2 and DQ−W_2 are very similar (17.8 and 18.8 kcal/mol, respectively) but somewhat less than that in 2-PYR−W_2 (20.32 kcal/mol). No corrections for basis set superposition errors[31] have been carried out, but the magnitude of these corrections should be very similar for the clusters of the same size. The similar binding energies of OI−W_n and DQ−W_n clusters of the same size confirms again that the water bridge can accommodate itself to modest changes in the *cis*-amide group with little loss in binding. The fact that their binding energies differ from those computed for 2-PYR−W_n, despite the similar donor−acceptor distances in DQ and 2-PYR most likely reflects the differences in electronic structure. 2-PYR−W_1 may experience some strengthening of the H-bonds in the bridge due to the extended π system of which the NH and C═O groups are a part.

In the OI−W_n series, the incremental change in total binding energy with addition of each water molecule to the bridge is nonmonotonic, varying from 8.0 to 9.8 to 8.2 kcal/mol. This probably reflects the better fit of the water dimer bridge than either the W_1 (too short) or W_3 (too long) bridges.

The calculated, scaled (0.976) harmonic vibrational frequencies, infrared intensities, and normal mode descriptions of the hydride stretch vibrations of OI−W_{1-3} and DQ−$W_{1,2}$ are presented in Table 4.

C. Comparison between Experiment and Theory: *1. OI−W_1 and DQ−W_1.* The experimental IR spectra of OI−W_1 and DQ−W_1 are compared with calculated, scaled vibrational frequencies and infrared intensities for the water bridge structures in Figure 4. Not surprisingly, in both cases, there is good agreement between experiment and theory, confirming the H-bonded bridge as the structural motif for both complexes, as deduced already from the electronic spectroscopy[13] and by comparison with the 2-PYR−W_1 complex. The calculations can provide insight into two aspects of the spectra in the bridge fundamental region.

First, the form of the normal modes clarifies the source of the unequal intensities of the two bridge fundamentals in DQ−W_1 (Figure 4c,d). It was shown in the earlier study[12] of 2-PYR−W_1 that the two bridge fundamentals are not localized NH and OH stretches but instead are delocalized over the NH and OH oscillators. The same holds true in DQ−W_1. As shown in the vector diagrams in Figure 5a, since the NH and OH bonds are nearly antiparallel to each other, the higher-frequency bridge vibration in which the two XH groups oscillate out-of-phase with one another (i.e., one stretching, the other compressing) has an enhanced intensity since the two dipole derivatives add. At the same time, the lower-frequency, "in-phase" oscillation leads to a partial cancellation of dipole derivatives and a much weaker intensity, as observed.

Second, the experimental intensities of the two bridge fundamentals in OI−W_1 are quite different from those in DQ−W_1 and are also at variance with calculation (Figure 4a,b). The much larger intensity of the lower-frequency bridge fundamental suggests a significant change in the degree of OH/NH coupling in OI−W_1 that is not properly accounted for by the calculation. The degree of mixing between the OH and NH stretches depends sensitively on the energy separation of the local mode NH and OH ($\nu = 1$) levels in the absence of such coupling. Part of this difference between OI−W_1 and DQ−W_1 arises simply because in the OI monomer, the NH stretch is at 3493 cm^{-1}, nearly 50 cm^{-1} above that in DQ (3447 cm^{-1}) or 2-PYR (3438 cm^{-1}). As a result, a H-bonded water bridge of comparable strength in OI and DQ will lead to different degrees of OH/NH mixing.

Note that despite the fact that the NH stretches in 2-PYR and DQ occur at very similar frequencies, the pair of hydrogen-bonded stretch fundamentals in 2-PYR−W_1 is found at lower frequency. This is consistent with the larger binding energy calculated for the conjugated 2-PYR−W_1 complex.

The experimental spectra of Figure 4a,c both possess weak combination bands built off the free OH stretch. In OI−W_1, this combination band appears at 3792 cm^{-1}, corresponding to a 67 cm^{-1} intermolecular vibration. The calculations find an out-of-plane intermolecular bend of the water molecule with a scaled frequency of 48 cm^{-1} that is a reasonable candidate. In the S_1 state, this vibration has been observed at 47 cm^{-1} and assigned to the out-of-plane bend.[13] In the ground-state IR spectrum, the combination band involving this vibration probably gains intensity through the large-amplitude motion associated with the vibration reorienting the oscillating free OH dipole, much as occurs in the nonrigid benzene−water complex.[17] An analogous band is found in the DQ−W_1 spectrum at 3780 cm^{-1}, 56 cm^{-1} above the free OH stretch.

The weak, sharp band at 3606 cm^{-1} in the OI−W_1 spectrum is tentatively assigned as a second intramolecular/intermolecular combination band built off one of the bridge fundamentals. Its separation from the higher frequency bridge fundamental is 169 cm^{-1}, close to the calculated frequency for the intermolecular stretch of 180 cm^{-1}. If this assignment is correct, the sharpness

TABLE 4: Calculated Harmonic Vibrational Frequencies, Infrared Intensities, and Mode Descriptions for OI−W$_n$ (n = 0−3), DQ−W$_n$ (n = 1, 2), and Water Monomer in the Hydride Stretch Region of the Infrared

		freq shift (cm^{-1})		
freq[a] (cm^{-1})	int (KM/mol)	NH[b]	OH[c]	normal mode description[d]
				W$_1$
3638	7		−60	SS
3759	53		+60	AS
				OI
2992	6			SS: CH_2
3026	3			AS: CH_2
3109	5			aromatic CH stretch
3114	6			aromatic CH stretch
3125	24			aromatic CH stretch
3136	18			aromatic CH stretch
3547	41	0		free NH stretch
				DQ
3502	25	0		free NH stretch
				OI−W$_1$
3387	92	−160	−311	NH (69) + W1 HB OH (31)
3437	591	−109	−261	NH (32) − W1 HB OH (68)
3725	86		27	W1 free OH stretch
				DQ−W$_1$
3352	98	−150	−346	NH (74) + W1 HB OH (26)
3418	590	−84	−280	NH (26) − W1 HB OH (74)
3723	83		25	W1 free OH stretch
				OI−W$_2$
3206	463	−340	−492	NH (62) + W1 HB OH (24) + W2 HB OH (14)
3303	891	−244	−396	NH (24) − W1 HB OH (44) − W2 HB OH (32)
3362	1163		−336	W1 HB OH (41) − W2 HB OH (59)
3716	68		18	W1 free OH
3721	100		23	W2 free OH
				DQ−W$_2$
3217	367	−285	−481	NH (62) + W1 HB OH (24) + W2 HB OH (14)
3305	729	−197	−393	NH (24) − W1 HB OH (45) − W2 HB OH (31)
3367	1217		−331	W1 HB OH (41) − W2 HB OH (59)
3713	58		15	W1 free OH
3725	106		27	W2 free OH
				OI−W$_3$
3192	489	−355	−506	NH (41) + W1 HB OH (28) + W2 HB OH (21) + W3 HB OH (10)
3254	1295	−293	−444	NH (35) − W1 HB OH (21) − W2 HB OH (34) − W3 HB OH (10)
3309	1083	−237	−389	NH (9) − W1 HB OH (44) + W2 HB OH (32) + W3 HB OH (15)
3375	1098		−323	W2 HB OH (33) − W3 HB OH (67)
3710	60		12	W1 free OH stretch
3715	69		17	W2 free OH (83) − W3 free OH (17)
3717	121		18	W2 free OH (17) + W3 free OH (83)

[a] Calculated frequencies are scaled (scaling factor = 0.976). [b] NH frequency shifts are relative to the calculated, scaled free NH stretch of OI (3547 cm^{-1}) or DQ (3502 cm^{-1}). [c] OH frequency shifts are relative to the calculated, scaled average of the symmetric and antisymmetric stretches of water monomer (3698 cm^{-1}) at the Becke3LYP/6-31+G*(5d) level of theory. [d] CH_2 = OI CH_2 group; AS = antisymmetric stretch; SS = symmetric stretch; NH = N−H group of OI or DQ; HB = hydrogen-bonded. Water molecules are numbered in the order they appear from the NH to the C=O group of oxindole in the hydrogen-bonded bridge. The percentage of each component of the bridge XH groups that contribute to the normal modes is given in parentheses when a local mode is not sufficient to describe the motion. Small contributions from other motions (e.g., the free OH stretch in OI−W$_1$) have not been included.

of the band is surprising, since it is built off a broad bridge fundamental.

Finally, a close inspection of the experimental spectrum in Figure 4a shows a small *gain* signal with relative frequencies, intensities, and widths that mirror those found in the two intense bridge fundamentals in OI−W$_2$. It appears that absorption of an infrared photon by OI−W$_2$ leads to fragmentation of the cluster to OI−W$_1$ + W. This OI−W$_1$ fragment must have a small enough excess energy that it produces an OI−W$_1$ R2PI signal in the region of the cold OI−W$_1$ $S_1 \leftarrow S_0$ origin, producing the observed gain signal.

2. OI−W$_2$ and DQ−W$_2$. The experimental RIDIR spectrum of OI−W$_2$ and DQ−W$_2$ are compared with the calculated vibrational frequencies and infrared intensities in Figure 6. There is an excellent one-for-one correspondence between calculation and experiment for both clusters, confirming the earlier conclusion that they both have structures in which water dimer bridges span the *cis*-amide group, as shown in the insets of Figure 6b,d.

The calculated form of the hydride stretch normal modes for OI−W$_2$ is shown in Figure 5b. All three bridge fundamentals are quite delocalized but have dominant contributions from one of the XH oscillators, beginning with the NH bond in the lowest frequency fundamental (B1) and shifting along the bridge as the frequency increases (B2 and B3). As before, the lowest frequency bridge fundamental (B1) is an in-phase oscillation

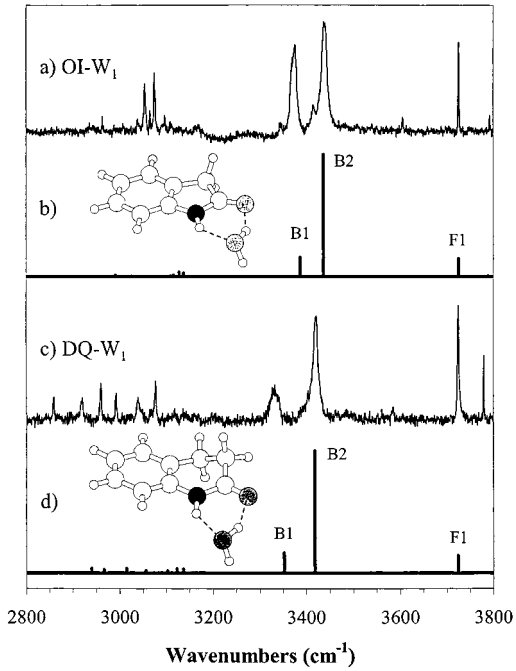

Figure 4. Comparison of the RIDIR spectra of OI−W_1 (a) and DQ−W_1 (c) with the scaled, harmonic vibrational frequencies and infrared intensities of the lowest energy structures calculated for OI−W_1 (b) and DQ−W_1 (d) by DFT/Becke3LYP calculations with the 6-31+G* basis set. Scaling factor = 0.976. Pictures of the calculated structures are provided as insets next to their respective stick spectra. The color coding, which is used in this and subsequent figures, is as follows: black spheres represent nitrogen, gray spheres represent oxygen, large white spheres represent carbon, and small white spheres represent hydrogen. The calculated hydride stretch bridge fundamentals are labeled B1 and B2, while the free OH stretch is labeled F1. See Table 3 and Figure 7 for descriptions of these normal modes.

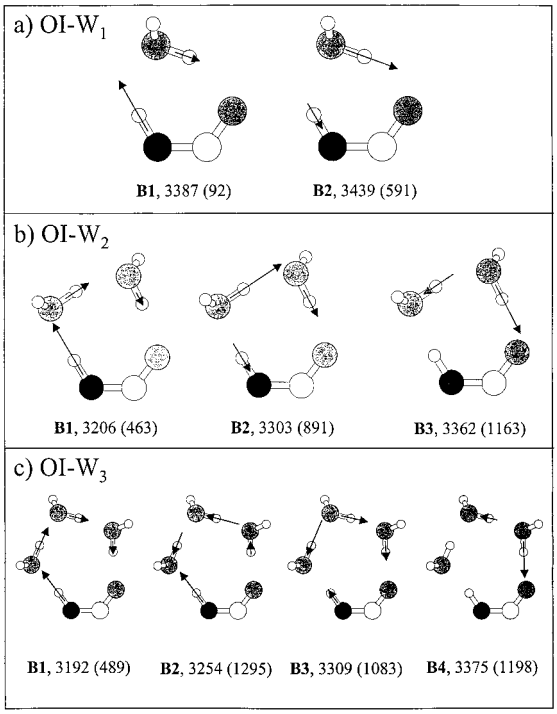

Figure 5. Pictorial representation of the calculated normal modes of the NH and OH stretch vibrations for OI−W_1 (a), OI−W_2 (b), and OI−W_3 (c). The direction and magnitude of each contributing motion is represented by arrows. The description (B1, B2, etc.), scaled frequency (in reciprocal centimeters)), and IR intensity (shown in parentheses) of each mode is added below its corresponding picture. The pictures demonstrate the strong mixing of the hydrogen-bonded stretches within each bridge.

of all three XH groups in the bridge, leading to partial cancellation of the bond dipoles and weakening its intensity relative to the other fundamentals. A comparison of the bridge fundamentals of OI−W_2, DQ−W_2, and 2-PYR−W_2 (best seen in Figure 3) shows that the intensity of this lowest frequency fundamental is smallest in OI, intermediate in DQ, and largest in 2-PYR. The changing intensity of this band probably reflects differences in the form of this mode due to different degrees of mixing of the XH oscillators in the bridge.

The two free OH stretches in OI−W_2 and DQ−W_2 are calculated as localized on individual water molecules, with the NH-bound water having a slightly lower frequency than the carbonyl-bound water. The experimental free OH stretch region of DQ−W_2 (Figure 6c) shows this distinction among the free OH fundamentals. If the calculations are correct, one would tentatively assign the band at 3712 cm^{-1} to the NH-bound water and that at 3721 cm^{-1} to the carbonyl-bound water. Surprisingly, in OI−W_2 (Figure 6a), the free OH stretch region consists of a triplet of transitions rather than the expected doublet. One possible explanation of the additional transition is that it arises from a tunneling splitting due to the flipping coordinate.

Two weak transitions at 3487 and 3565 cm^{-1} in the spectrum of OI−W_2 are each approximately 170 cm^{-1} above the two strong bridge fundamentals at 3329 and 3391 cm^{-1}, respectively. The calculations predict that the intermolecular stretches of the two water molecules are at 170 and 191 cm^{-1}, suggesting that the observed transitions are combination bands between the bridge fundamentals and the intermolecular stretches.

3. OI−W_3. The experimental RIDIR spectrum for OI−W_3 is compared with the calculated spectrum for the W_3 bridge in Figure 7. Both experiment and theory show the unmistakable spectral signature of bridge formation that clumps all the intense, broadened H-bonded bridge fundamentals in the 3200−3400 cm^{-1} region. According to the calculations, the bridge vibrations are extensively delocalized over all XH oscillators in the bridge. Table 4 gives the percent character of each normal mode in parentheses in the column that describes the normal modes. The amide NH group localizes more in the low-frequency bands (B1 and B2), while the water that is bound to the carbonyl group (W3) dominates the highest frequency bridge fundamental (B4).

It is tempting to make a one-for-one match-up between calculated and experimental bands in the bridge fundamental region. However, the possible contribution of Fermi resonances, particularly with the overtones of the water bends, when coupled with the considerable widths of the experimental bands, makes such a correlation tentative at best.

At the HF/6-31G** level of theory, a second OI−W_3 structure was found only 0.4 kcal/mol above the bridge global minimum. This structure is similar to one found recently by Robertson et al.[31] for *N*-benzylformamide−W_3. In it, a third water molecule is added to the OI−W_2 bridge structure in such a way as to form a W_3 cycle, accepting an H-bond from the amide-bound water and donating an H-bond to the carbonyl-bound water.[13] In so doing, the amide-bound water becomes a double-donor, single-acceptor water. The calculated hydride stretch vibrational frequencies of this structure are incompatible with experiment, especially those of the double-donor water, which are much too high in frequency. Furthermore, no minimum corresponding to this structure could be found at the DFT Becke3LYP/6-31+G* level of theory.

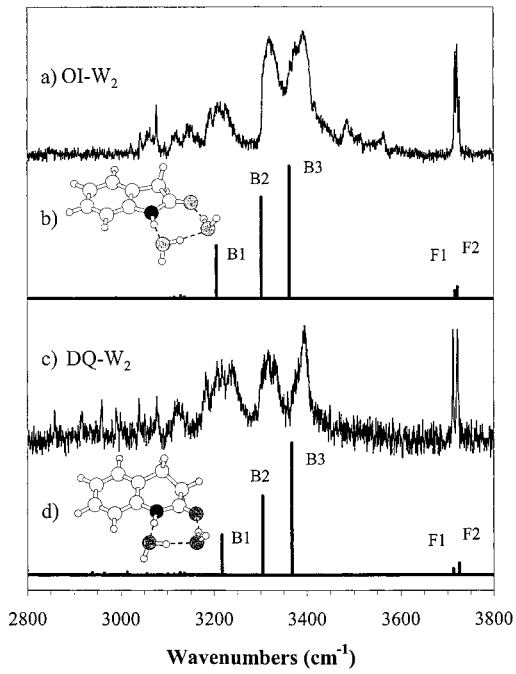

Figure 6. Comparison of the RIDIR spectra of OI−W_2 (a) and DQ−W_2 (c) with the scaled, harmonic vibrational frequencies and calculated infrared intensities of the lowest energy structure calculated for OI−W_2 (b) and DQ−W_2 (d) by DFT/Becke3LYP calculations with the 6-31+G* basis set. Scaling factor = 0.976. Pictures of the calculated structures are provided as insets next to their respective stick diagrams. The calculated hydride stretch fundamentals are labeled B1−B3, F1, and F2. See Table 3 and Figure 7 for descriptions of these normal modes.

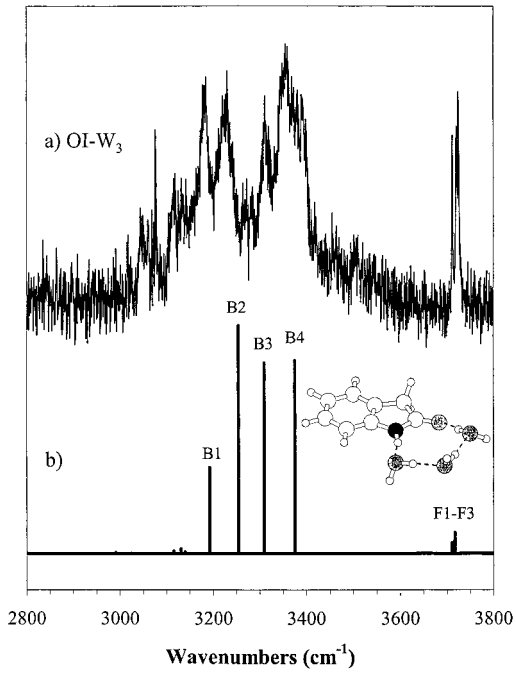

Figure 7. Comparison between the RIDIR spectrum of OI−W_3 (a) and its corresponding calculated harmonic vibrational frequencies (b). A picture of the calculated structure is included as an inset. The calculated hydride stretch fundamentals are labeled B1−B4 and F1−F3. See Table 3 and Figure 7 for descriptions of these normal modes.

IV. Discussion and Conclusions

A. Preference for Water Bridges across the *cis*-Amide Group. This study of OI−W_n and DQ−W_n clusters with n = 1−3 has shown that the water bridges formed between the N−H and C═O sites in 2-PYR are a general binding motif for water to the *cis*-amide group. This was anticipated already from the R2PI spectroscopy[13] but is unambiguously confirmed by the RIDIR spectra presented in this paper. The single-molecule bridge is somewhat too short for the purpose, leading to bent and somewhat elongated N−H···O and O−H···O═C H-bonds. According to the calculations, the water bridge actually causes a small flexing of the *cis*-amide NH in toward the C═O in seeking to strengthen the water molecule's H-bonds to both groups. In the water dimer bridge, the match in size is much better, although in this case the water dimer is slightly too large to fit into the *cis*-amide jaw. In the presence of the water dimer, the *cis*-amide NH bond flexes out slightly to accommodate the water dimer. At the same time, the water dimer is squeezed between the NH and C═O groups to a separation of about 2.70 Å, almost 0.3 Å less than that in the free water dimer, due in large measure to the cooperative strengthening that accompanies completion of the bridge.

This preference for bridge over alternative structures extends to OI−W_3, despite the fact that the bridge is substantially too long in this case. One of the design features of the water bridge is its inherent flexibility. In OI−W_3, this flexibility enables the W_3 bridge to slide and buckle in such a way as to maintain strong, near-linear H-bonds that terminate without loss of strength at the N−H and C═O sites.

B. IR Spectral Signatures of the Bridges. The hydride stretch infrared spectra of the water bridges across the *cis*-amide linkage show a clear division of the infrared fundamentals into sharp, weak free OH stretches just above 3700 cm^{-1} and strong, broadened bands due to the bridge XH fundamentals appearing in the 3200−3450 cm^{-1} region. This is similar to what is observed in *cyclic*, H-bonded clusters where the division is into free and single-donor OH groups. However, in the presence of the *cis*-amide H-bonding sites, formation of a bridge can occur even when only one or two water molecules are present, before cyclization of the solvent is possible. Furthermore, there is clear involvement of both NH and C═O groups in the H-bonding. The shift of the NH stretch fundamental into the bridge region is a signature that the NH does indeed serve as a H-bond donor to water in the clusters. The involvement of the carbonyl acceptor site is seen indirectly in the number and wavenumber position of the H-bonded OH stretch fundamentals, one of which is bound to the C═O group. The carbonyl group is involved in cooperative strengthening of the water OH fundamentals, which shifts the bridge fundamentals to 3400 cm^{-1} and below. The carbonyl group also shifts the XH group(s) in the bridge into resonance with one another, inducing strong coupling between them, which influences their relative intensities significantly.

The cooperative strengthening of the H-bonds in the bridge is seen already in OI−W_1, where the coupled NH/OH fundamentals appear at 3375 and 3437 cm^{-1} (Figure 5), almost 100 cm^{-1} lower in frequency than complexes in which water binds to a carbonyl alone. For instance, tropolone−W_1 has a H-bonded OH stretch at 3506 cm^{-1},[33] while the carbonyl-bound isomer of *trans*-formanilide−W_1 is a Fermi resonant split doublet at 3515 and 3536 cm^{-1}.[34]

The delocalization of the bridge vibrations among the XH groups results because the water bridge OH and H-bonded amide NH stretches are at similar frequencies, opening the way for extensive mixing between them. It is somewhat surprising that the H-bonded amide NH stretch appears in the same region as the H-bonded water OH stretches, since the uncomplexed *cis*-amide NH fundamental is over 200 cm^{-1} lower in frequency

than the free OH stretch of water. In OI−W_1, the bridge fundamentals at 3437 and 3375 cm^{-1} are shifted by 56 and 118 cm^{-1}, respectively, from the oxindole monomer NH stretch (3493 cm^{-1}) but are shifted 278 and 340 cm^{-1} from the free OH stretch of water (∼3715 cm^{-1}). The greater frequency shift of the water OH than the amide NH group is probably because the amide NH is a H-bond donor located at the beginning of the bridge, while the water OH is both a donor and acceptor in the bridge.[27]

The similarities between the *cis*-amide−W_2 cluster and the cyclic W_3 cluster extend beyond the simple break-up into free OH stretch and H-bonded OH stretch vibrations with a large gap between. Both the frequency patterns and the relative intensities of the bridge fundamentals are very similar as well.

In the cyclic water trimer, the H-bonded OH stretch fundamentals consist of a degenerate set of modes at higher frequency that carry all the oscillator strength and a dipole-forbidden transition at lower frequency.[14,35] In the presence of a perturber (such as benzene) the degeneracy of the higher frequency vibrations is broken, and the lower-frequency band gains some intensity.[14] This is precisely the pattern recognizable in the bridge fundamentals of OI−W_2 (Figure 6a) in which the two higher frequency vibrations carry most of the oscillator strength and are split by a small amount relative to the much weaker, lower frequency bridge fundamental. This intensity distribution is less clear in 2-PYR−W_2 and DQ−W_2, where the slightly smaller distance between NH and C═O groups must change somewhat the structure and degree of coupling along the bridge.

The similarity of the spectra of the W_3 cycle and OI−W_2 bridge simply reflects a similar form for the normal modes in the two contexts (Figure 5b); namely, a set of near-degenerate single-node longitudinal phonons at higher frequency (B2 and B3) and a nodeless (i.e., in-phase) oscillation of all three XH groups in the lowest frequency vibration (B1), in which the directions of the oscillating dipoles partially cancel one another.[34] In essence, the carbonyl oxygen atom and amide NH together play the role of a single water molecule in the cyclic water trimer. The amide group, with its donor and acceptor sites in close proximity to one another, undergoes and enables a cooperative strengthening much as a single water molecule does when incorporated into a H-bonded cycle.

Finally, it is worth commenting briefly on the dependence of the observed frequencies and infrared intensities on the nature of the *cis*-amide group to which the W_n bridge is attached. The *cis*-amide group is incorporated into a five-membered ring with larger H(N)−(C)O distance in OI, a six-membered ring with significant strain in DQ, and a six-membered pseudoaromatic ring in 2-PYR. The comparisons shown in Figures 2 and 3 show more similarity than difference between the spectra of the three molecules, as one might expect if the water bridges themselves adjust to small changes in the separation, orientation, or electronic structure of the bridge termination sites with little loss in net binding strength. However, there is a slight shift to lower frequency of the bridge fundamentals in DQ over OI, which is consistent with a slight strengthening of the bridge in a six-membered ring over a five-membered ring. A further, more substantial shift is observed in the 2-PYR−W_1 spectrum, particularly in the higher frequency XH stretch, largely due to the XH attached to the C═O group. This carries over to the W_2 bridges as well, where the frequency of the OH···O═C fundamental is substantially lower in 2-PYR than in DQ or OI. This is consistent with a strengthening of the bridge at the C═O end when the C═O group is incorporated into an extended π system, as it is in 2-PYR.

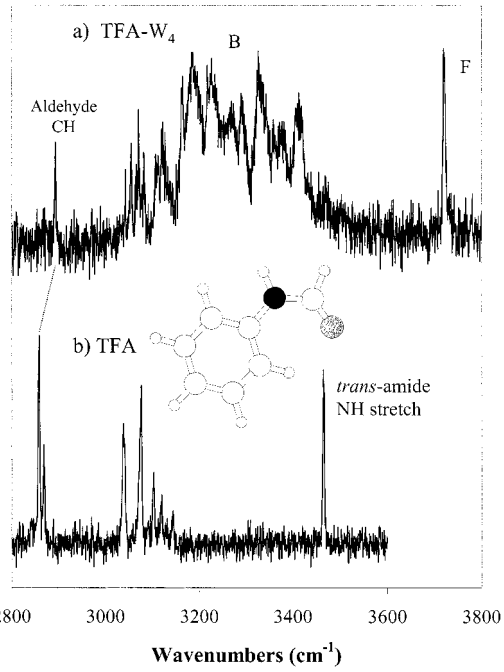

Figure 8. Comparison between the RIDIR spectra of *trans*-formanilide (TFA) (b) and TFA−W_4 (a). The structure of this water-containing cluster has been previously determined (refs 5 and 6) to be a W_4 bridge, connecting the NH and C═O functional groups of the amide. A picture of the calculated structure of TFA showing its *trans*-amide group is included as an inset.

The intensity changes along the series are more difficult to understand in detail, as noted earlier, since the form of the bridge normal modes depends quite sensitively on the extent of coupling of the XH bonds in the bridge. This coupling strength likely has as much to do with the changing monomer NH frequencies as on the bridge itself.

It would also be of interest to better understand the changes induced by water bridge formation on the *cis*-amide group itself. However, the XH stretch infrared spectra are not particularly sensitive to these changes, pointing to the need for Raman or infrared spectra in the region of the amide fundamentals.[2,3] Rotationally resolved studies would also be helpful in this regard.

C. Longer Bridges. In the *cis*-amide group, the donor N−H and carbonyl oxygen lone pair acceptor sites are adjacent to one another but are oriented in such a way that H-bonds to them produce an arched water bridge. It will be interesting to study the spectroscopy of H-bonded bridges in other situations. In general, one anticipates water bridges between donor and acceptor sites to take on shapes and strengths dictated by the relative orientation of the donor and acceptor sites and the match between the natural length of the water bridge and the distance between the bridge termination sites. This distance match-up will determine how stretched or buckled the water bridge must be to reach between the sites, which in turn will influence the frequencies and intensities of the bridge fundamentals.

The *trans*-formanilide−$(water)_4$ cluster, whose RIDIR spectrum is shown in Figure 8, is one such longer bridge formed under quite different circumstances. On the basis of its R2PI spectrum, *trans*-formanilide−$(water)_4$ (hereafter TFA−W_4) has recently been assigned as a four-molecule water bridge that spans the *trans*-amide group by Dickinson et al.[5] and Fedorov and Cable.[6] Very recently, Robertson[34] confirmed this structure by IR−UV ion-dip spectroscopy. In that work, extensive calculations were also carried out on various potential structures for TFA−W_4, including the vibrational frequencies and infrared

intensities. These calculations showed that a H-bonded W_4 bridge stretched between NH and C═O was most consistent with the experimental data in the H-bonded stretch region. Our group has also recorded the spectrum of TFA−W_4 as a part of the present study, which is reproduced in Figure 8a. Over the region of overlap (3000−3800 cm^{-1}), the spectra from the two groups are identical. Like OI−W_3, the spectrum of TFA−W_4 consists of free OH stretch transitions above 3700 cm^{-1}, a large gap, and a clump of similar-intensity bridge fundamentals in the 3200−3400 cm^{-1} region. In addition, the spectra of Figure 8 extend down to 2800 cm^{-1}, where the aldehyde's CH stretch absorption appears. In TFA−W_4, this band is at 2893 cm^{-1}, shifted from its frequency in the TFA monomer (Figure 8b) by +34 cm^{-1}. In TFA−W_n clusters, the spatial separation of the NH and C═O groups makes it possible to observe clusters in which water molecule(s) bind either at the NH or C═O groups. It is observed that the carbonyl-bound TFA−W_n clusters with $n = 1$ and 2 undergo characteristic shifts in the aldehyde CH stretch toward higher frequency (by +31 and +68 cm^{-1}, respectively). The fact that the aldehyde CH stretch in TFA−W_4 undergoes a similar blue shift indicates that the W_4 subunit does indeed reach across the *trans*-amide structure to donate a H-bond to the carbonyl group, likely with one of the waters in the bridge accepting a weak H-bond from the aldehyde CH group.

The close similarity of the spectra of TFA−W_4 (Figure 8) and OI−W_3 (Figure 7) suggests, then, that TFA−W_4 shares with OI−W_3 its NH···W_n···O═C bridge structure. Given this fact, it is worth noting that the OI−W_2, OI−W_3, and TFA−W_4 spectra all have bridge fundamentals appearing in the same frequency range; that is, there is little additional shift in the frequency of the bridge fundamentals as the length of the bridge is increased from two to four water molecules. It would seem, then, that the cooperative strengthening of the water bridge is quite localized to the H-bonding sites on either side of a given water, and hence tends to depend only weakly on the overall length of the bridge once the bridge can span the donor−acceptor gap. This is in keeping with the calculations of H-bonded chains of water molecules by Ojamäe and Hermansson.[27]

D. Revisiting the Broadening of the Bridge Fundamentals. As a motivation for this work, the introduction described the unusual breadths of the bridge fundamentals in 2-PYR−W_n and 2-hydroxypyridine−W_n (2-HP−W_n), which are tautomers of one another.[12] There the possibility existed that the broadening could be influenced by water-mediated tautomerization via a concerted H-atom transfer along the bridge following excitation of hydride stretch vibrations closely associated with the reaction coordinate. In OI and DQ, such tautomerization routes are not energetically accessible, yet the spectra show similar breadths to those in 2-PYR−W_n, as demonstrated in Figure 6. As a result, it appears that the broadening of the bridge fundamentals is a general feature of the strong, H-bonded bridges formed across the *cis*-amide group. As noted earlier,[12] this broadening must result from unusually large anharmonic couplings of the XH stretch vibrations in the bridge with bath states of undetermined makeup. In particular, an unusually strong coupling along the bridge may accompany the squeezing of the water dimer and the cooperative strengthening of the H-bonds in forming the bridge. In a time-dependent picture of the vibrational redistribution, following vibrational excitation, the XH oscillation could quickly dissipate into bends and stretches of the bridge that relieve this strain or even break one of the bonds in the bridge.

In addition to the broadening of individual bands that characterizes the spectra studied in this paper, there are circumstances in which strongly H-bonded XH oscillators are involved in extensive Fermi resonant mixing with a relatively sparse set of dark states.[36] This leads to a sharing of the XH stretch oscillator strength by a number of discrete bands distributed over several hundred wavenumbers, each of which individually may have considerable breadth. In work to be reported elsewhere, the amide NH stretch fundamentals of OI and DQ display just such an effect when they are shifted to well below 3200 cm^{-1} by strong H-bonds with ammonia or another oxindole molecule. Under such circumstances, it can be difficult even to identify the amide NH stretch fundamental in the midst of the Fermi resonant states that borrow oscillator strength from it.

Acknowledgment. We gratefully acknowledge the support of the National Science Foundation Experimental Physical Chemistry program under Grants CHE-9728636 and CHE-9727527.

References and Notes

(1) Zwier, T. S. *Annu. Rev. Phys. Chem.* **1996**, *47*, 205−241.
(2) Torii, H.; Tasumi, M. *Infrared Spectroscopy of Biomolecules*; Wiley: New York, 1996; p 1.
(3) Torii, H.; Tatsumi, T.; Tasumi, M. *J. Raman Spectrosc.* **1998**, *29*, 537−546, and references therein.
(4) Jeffrey, G. A.; Saenger, W. *Hydrogen Bonding in Biological Structures*; Springer-Verlag: New York, 1991.
(5) Dickinson, J. A.; Hockridge, M. R.; Robertson, E. G.; Simons, J. P. *J. Phys. Chem. A* **1999**, *103*, 6938−6949.
(6) Fedorov, A. V.; Cable, J. R. *J. Phys. Chem. A* **2000**, *104*, 4943−4952.
(7) Trembreull, R.; Sin, C. H.; Pang, H. M.; Lubman, D. M. *Anal. Chem.* **1985**, *57*, 2911.
(8) Nimlos, M. R.; Kelley, D. F.; Bernstein, E. R. *J. Phys. Chem.* **1989**, *93*, 643−651.
(9) Held, A.; Pratt, D. W. *J. Am. Chem. Soc.* **1993**, *115*, 9708−9717.
(10) Matsuda, Y.; Ebata, T.; Mikami, N. *J. Chem. Phys.* **1999**, *110*, 8397−8407.
(11) S. Leutwyler, private communication.
(12) Florio, G. M.; Gruenloh, C. J.; Quimpo, R. C.; Zwier, T. S. *J. Chem. Phys.* **2001** (in prepartion).
(13) Fedorov, A. V.; Cable, J. R., in prepartion.
(14) Zwier, T. S. The Infrared spectroscopy of hydrogen-bonded clusters: Cycles, chains, cubes, and three-dimensional networks. In *Advances in Molecular Vibrations and Collision Dynamics*; Bowman, J. M., Bacic, Z., Eds.; JAI Press: Greenwich, CT, 1998; Vol. 3, pp 249−280.
(15) A. Fedorov, J. R. Carney, J. R. Cable, and T. S. Zwier, manuscript in preparation.
(16) Gotch, A. J.; Zwier, T. S. *J. Chem. Phys.* **1992**, *96*, 3388−3401.
(17) Pribble, R. N.; Garrett, A. W.; Haber, K.; Zwier, T. S. *J. Chem. Phys.* **1995**, *103*, 531−544.
(18) Page, R. H.; Shen, Y. R.; Lee, Y. T. *J. Chem. Phys.* **1988**, *88*, 5362−5376.
(19) Ebata, T.; Fujii, A.; Mikami, N. *Int. Rev. Phys. Chem.* **1998**, *17*, 331−362.
(20) Imhof, P.; Roth, W.; Janzen, C.; Spangenberg, D.; Kleinermanns, K. *Chem. Phys.* **1999**, *242*, 141−151.
(21) Palmer, P. M.; Chen, Y.; Topp, M. R. *Chem. Phys. Lett.* **2000**, *318*, 440−447.
(22) Buchhold, K.; Reimann, B.; Djafari, S.; Barth, H. D.; Brutschy, B.; Tarakeshwar, P.; Kim, K. S. *J. Chem. Phys.* **2000**, *112*, 18484−1858.
(23) Becke, A. D. *J. Chem. Phys.* **1993**, *98*, 5648.
(24) Lee, C.; Yang, W.; Parr, R. G. *Phys. Rev. B* **1988**, *37*, 785.
(25) Frisch, M. J.; Pople, J. A.; Binkley, J. S. *J. Chem. Phys.* **1984**, *80*, 3265.
(26) Frisch, M. J.; Trucks, G. W.; Schlegel, H. B.; Scuseria, G. E.; Robb, M. A.; Cheeseman, J. R.; Zakrzewski, V. G.; Montgomery, J. A., Jr.; Stratmann, R. E.; Burant, J. C.; Dapprich, S.; Millam, J. M.; Daniels, A. D.; Kudin, K. N.; Strain, M. C.; Farkas, O.; Tomasi, J.; Barone, V.; Cossi, M.; Cammi, R.; Mennucci, B.; Pomelli, C.; Adamo, C.; Clifford, S.; Ochterski, J.; Petersson, G. A.; Ayala, P. Y.; Cui, Q.; Morokuma, K.; Malick, D. K.; Rabuck, A. D.; Raghavachari, K.; Foresman, J. B.; Cioslowski, J.; Ortiz, J. V.; Stefanov, B. B.; Liu, G.; Liashenko, A.; Piskorz, P.; Komaromi, I.; Gomperts, R.; Martin, R. L.; Fox, D. J.; Keith, T.; Al-Laham, M. A.; Peng, C. Y.; Nanayakkara, A.; Gonzalez, C.; Challacombe, M.; Gill, P. M. W.; Johnson, B. G.; Chen, W.; Wong, M. W.; Andres, J. L.; Head-Gordon,

M.; Replogle, E. S.; Pople, J. A. *Gaussian 98*, revision A.7; Gaussian, Inc.: Pittsburgh, PA, 1998.
(27) Ojamae, L.; Hermansson, K. *J. Phys. Chem.* **1994**, *98*, 4271−4282.
(28) Dyke, T. R.; Muenter, J. S. *J. Chem. Phys.* **1974**, *60*, 2929−2930.
(29) Viant, M. R.; Cruzan, J. D.; Lucas, D. D.; Brown, M. G.; Liu, K.; Saykally, R. J. *J. Phys. Chem. A* **1997**, *101*, 9032−9041.
(30) Schütz, M.; Klopper, W.; Luthi, H. P.; Leutwyler, S. *J. Chem. Phys.* **1996**, *103*, 6114−6126.
(31) Robertson, E. G.; Hockridge, M. R.; Jelfs, P. D.; Simons, J. P. *J. Phys. Chem. A* **2000**, *104*, 11714−11724.
(32) Boys, S. F.; Bernardi, F. *Mol. Phys.* **1970**, *19*, 553.
(33) Frost, R. K.; Hagemeister, F. C.; Arrington, C. A.; Schleppenbach, D.; Zwier, T. S.; Jordan, K. D. *J. Chem. Phys.* **1996**, *105*, 2605−2617.
(34) Robertson, E. G. *Chem. Phys. Lett.* **2000**, *325*, 299−307.
(35) Honegger, E.; Leutwyler, S. *J. Chem. Phys.* **1988**, *88*, 2582−2595.
(36) Marechal, Y. *J. Chem. Phys.* **1987**, *87*, 6344−6353.